Aquatic Botany 106 (2013) 14–19

Contents lists available at SciVerse ScienceDirect

Aquatic Botany

journal homepage: www.elsevier.com/locate/aquabot

Probabilistic mapping of *Posidonia oceanica* cover: A Bayesian geostatistical analysis of seabed images

D. March*, J. Alós, M. Cabanellas-Reboredo, E. Infantes, M. Palmer

Instituto Mediterráneo de Estudios Avanzados, IMEDEA (UIB-CSIC), Miquel Marqués 21, 07190 Esporles, Islas Baleares, Spain

ARTICLE INFO

Article history:
Received 24 August 2011
Received in revised form 26 October 2012
Accepted 17 December 2012
Available online 7 January 2013

Keywords:
GIS
Seagrass
Marine parks
Geographical distribution
Bayesian hierarchical model
Benthic mapping
Wave exposition
Longitude: 2°40′E–2°48′E
Latitude: 39°23′N–39°31′N

ABSTRACT

A spatially-explicit predictive model was developed for the cover of the seagrass *Posidonia oceanica* in a marine protected area (MPA) at Palma Bay (NW Mediterranean). A low-cost, novel drop camera system was designed and used to acquire standardized images that were used for estimating *P. oceanica* cover. A simple, semi-quantitative cover index through visual inspection allowed robust estimates that are free of between-observer bias. A Bayesian kriging approach was implemented through a hierarchical model for non-Gaussian data. The map that was produced is a good match to a previous map of the presence–absence of *P. oceanica* that was produced by combining side scan sonar and aerial photography. The influence of bathymetry, near-bottom orbital velocities (U_b) and slope on cover distribution were evaluated using a generalized linear model, while taking into account the spatial dependence between observations. We found that the important environmental variables were depth and U_b, while no effect of slope was found. The approach used here allowed us to not only map the cover of *Posidonica oceanica* but also to provide spatial-explicit information of prediction uncertainty.

1. Introduction

Benthic habitat mapping plays an important role in the conservation and management of seagrass meadows, especially within the context of marine protected areas (MPAs; Jordan et al., 2005; Stevens and Connolly, 2005; Grech and Coles, 2010). Underwater photography and videography have been demonstrated to be powerful tools for monitoring benthic communities, especially because they are non-destructive methods for species identification that can provide observations over large areas (Holmes et al., 2007). In addition, the development of small, remotely-deployed devices have overcome the main limitations of SCUBA divers and oceanographic vessels, allowing the monitoring of great expanses from small boats at low cost and high efficiency (Stevens and Connolly, 2005).

Different statistical approaches have been used for modeling the spatial distribution of seagrasses and for examining their relationships with different environmental variables (Kelly et al., 2001; Fonseca et al., 2002; Fourqurean et al., 2003; Bekkby et al., 2008). Statistical analysis of these data is challenging because of the existence of spatial autocorrelation. Kriging is a family of geostatistical methods that explicitly incorporate the spatial structure of the data. Different types of kriging have previously been used to map seagrasses, such as indicator kriging (Holmes et al., 2007; Kendrick et al., 2008) and ordinary kriging (Fourqurean et al., 2001; Zupo et al., 2006; Leriche et al., 2011). However, as pointed out by Holmes et al. (2007), geostatistical models usually assume a Gaussian distribution. However, the type of data usually available for mapping seagrass meadows is presence–absence, or percent cover, which are not necessarily conform a Gaussian distribution. Recently, the implementation of Bayesian kriging has been demonstrated to be a useful tool to incorporate spatial effects that result from spatial autocorrelation, even when dealing with non-Gaussian distributions (Banerjee et al., 2004).

We combine seabed images and geostatistical analysis for extensive beds of *Posidonia oceanica* (L.) off Mallorca (Spanish Mediterranean). This species is endemic in the Mediterranean Sea, where it is the dominant and most abundant seagrass species and forms extensive meadows on both soft and hard bottoms from the sea level down to 40 m (Duarte, 1991; Boudouresque et al., 2009). The current status of *P. oceanica* is especially critical because this long-lived species grows very slowly (Marbà and Duarte, 1998) and is very sensitive to natural and anthropogenic disturbances (Boudouresque et al., 2009). The specific goals of this study are (1) to present a standardized method for image acquisition from a drop camera that allows the estimation of seagrass cover using a semi-quantitative scale estimated by visual inspection; (2) to evaluate the effect of some key environmental variables on seagrass cover;

* Corresponding author. Fax: +34 971611761.
E-mail address: david.march@uib.es (D. March).

0304-3770/$ – see front matter © 2013 Elsevier B.V. All rights reserved.
http://dx.doi.org/10.1016/j.aquabot.2012.12.005

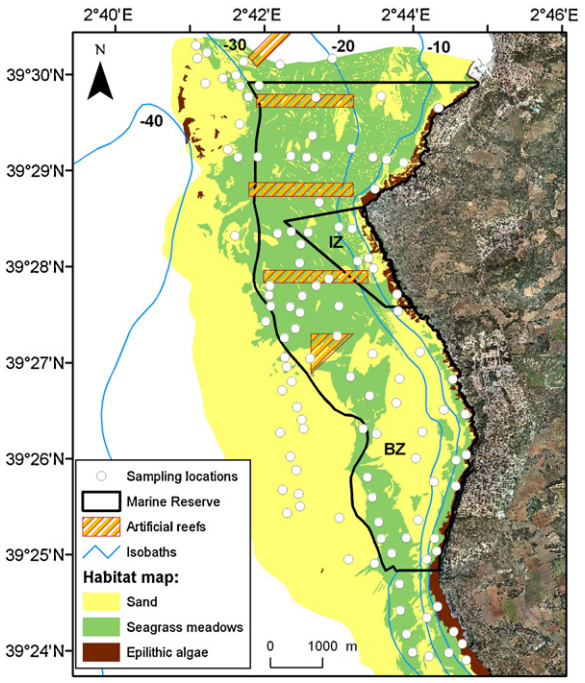

Fig. 1. Map of the study area showing the sampled locations. Palma Bay Marine Reserve (PBMR) boundaries enclose the Integral Zone (IZ) and the Buffer Zone (BZ). The location of the zones of artificial reefs in PBMR are presented.

(3) to generate a probabilistic map of seagrass cover that can be used as a proxy for the status of *P. oceanica* in a marine protected area (MPA) and 4) to incorporate uncertainty in the estimated maps of seagrass cover.

2. Materials and methods

2.1. Study area

Palma Bay Marine Reserve (PBMR) of Mallorca (NW Mediterranean) is a marine protected area (MPA) that covers an open water area between the shoreline and the 30 m isobath (Fig. 1). It was created in 1982, but human activities were not regulated in the reserve until 1999. This MPA is zoned into two management areas with different levels of protection: (1) an Integral Zone (~2 km^2), where all fishing activities, scuba diving, and boat anchoring over seagrass meadows are prohibited; and (2) a Buffer Zone (~24 km^2), where fishing activities and scuba diving are regulated, and boat anchoring is allowed everywhere. Since 1990, several artificial reefs have been deployed to dissuade furtive trawling in the area. Two main key habitats are represented in PBMR: seagrass meadows of *P. oceanica* and soft bottoms (Fig. 1).

2.2. Survey device and data collection

In this study, we measured seagrass cover using a customized prototype of a non-invasive drop camera system (Subcam, Albatros Marine Technologies S.L.) (Fig. 2). This system was used in a 5-m length motorboat and consisted of a video camera (SONY 1/3″ CCD, 3.6 mm lens, 1 lx/F 1.2) mounted on a metallic structure that allowed us to obtain vertical images at the same distance (148 cm) from the sea bottom. The area covered by the camera was 0.9 m^2. The camera was connected to an on-board computer via an umbilical cable (40 m length). Real-time images were visualized with custom software (Visualizer, Albatros Marine Technologies S.L.) that captured georeferenced images.

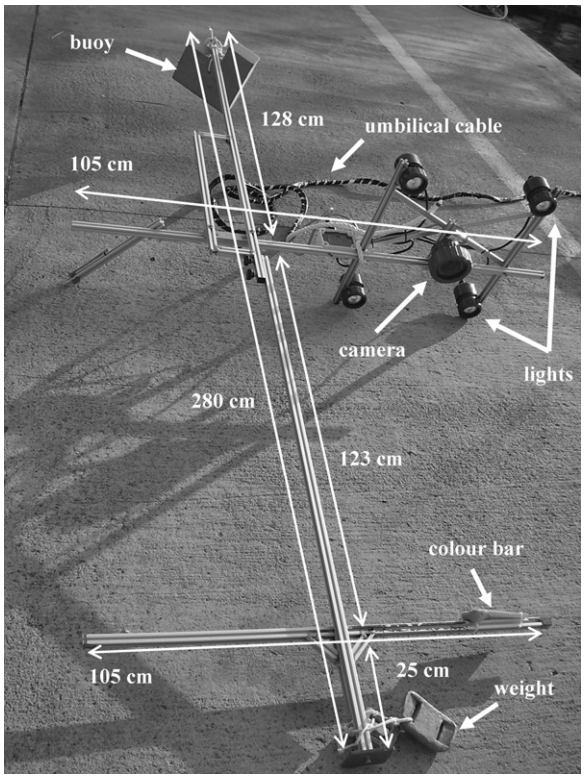

Fig. 2. Subcam (Albatros Marine Technologies S.L.) system. A video camera is mounted on a metallic structure to obtain standardized images of seagrass cover. The system is dropped from a small boat by an umbilical cable that permits obtaining real-time images.

We examined the data of 112 sampling locations from between 5 and 35 m depth, collected between May 2009 and June 2009 (Fig. 1). During this season, *P. oceanica* reaches its maximum leaf length (Fourqurean et al., 2007), which facilitated the identification of *P. oceanica* in localities of low cover. At each location, three images were captured in succession at random sampling positions separated between 2 and 10 m apart. We selected days with gentle winds to minimize boat drift. In total, we recorded 336 images. Each of these 336 images was manually processed for determining the cover of *P. oceanica* by three independent trained observers (see Subsection 2.5.1 for the assessment of the between-observer bias).

2.3. Quantification of seagrass cover

Image classification was based on the Braun-Blanquet Cover Abundance (BBCA) scale, previously used for seagrass research (Fourqurean et al., 2001, 2003). The BBCA assesses cover according to a scale that has 25% intervals with an additional low cover class up to 5% (Table 1). We then transformed the BBCA scores to the Average Covering Index (ACI), which assumes that each discrete value corresponds to the mean point of each class interval (Boudouresque, 1971; van der Maarel, 1979).

Table 1
Braun-Blanquet Cover Abundance (BBCA) scale and Average Covering Index (ACI). Each habitat type was scored in each image according to this scale.

BBCA scale	Interpretation	ACI (%)
0	Absence	0
1	<5% cover	2.5
2	5–25% cover	15
3	25–50% cover	37.5
4	50–75% cover	62.5
5	75–100% cover	87.5

The statistical unit for the foregoing analysis was the location. Therefore, first the three ACI scores of an image (one per observer) were averaged. Then, the averaged ACI scores of the three images from the same location were averaged again, to obtain a single ACI value per location.

2.4. Predictor variables

Three key environmental variables were selected a priori as putative explanatory variables of seagrass cover. We generated models for bathymetry, slope and near-bottom orbital velocities in the domain vegetated by *P. oceanica*, as determined by a previous map of benthic communities (*Posidonia*-LIFE map, Government of Balearic Islands). A digital bathymetric model (15 m × 15 m grid size) was created using original bathymetric contours provided every 1 m (Posidonia-LIFE map). We then computed the slope at the same resolution using the Spatial Analyst extension of ArcGIS 9.2 (ESRI).

Near-bottom orbital velocities (U_b) at the study area were calculated from wave conditions to quantify the wave exposition experienced by the seagrass meadow. As water waves propagate from deep to shallow water, they change their properties (wave length, wave height and direction), and therefore, deep water waves have to be propagated to shallow waters (area of interest) using a numerical model (Infantes et al., 2009, 2011; Álvarez-Ellacuria et al., 2010). Significant wave height (H_s), peak period (T_p) and direction were obtained from the closest WANA node (WANA2069035), located approximately 15 km from the study site at 50 m depth (2.625 E 39.375 N). The WANA node provides operationally wave data by the reanalysis of a third generation spectral WAM model.

The analysis of the wave data for the WANA node for the period 1996–2010 shows that, at the study area, the most energetic waves are from the SW, with an average H_s of 0.7 m and T_p of 5.5 s. These conditions were propagated to the shore using a numerical model based on the mild slope parabolic approximation (Kirby and Dalrymple, 1983). The model output provided a wave field for the whole grid and at the appropriate scale (15 m × 15 m grid size). Near-bottom orbital velocities (U_b) at the experimental locations were calculated from the wave propagation model outputs using linear wave theory (see Infantes et al., 2009 for details). This model does not take into account viscous effects such as the wave attenuation due to the presence of vegetation (Infantes et al., 2012), which could overestimate the values of the U_b where a dense seagrass meadow is present.

2.5. Data analysis

2.5.1. Observer bias

To assess between-observer differences, a set of preliminary trial and training sessions was completed based on a subset of images as a reference scale. Three observers then scored the cover of *P. oceanica* in all of the images. The existence of between-observer differences for ACI values on the five types of seabed considered was tested using an ANOVA. The data were not normal even after applying conventional transformations. Thus, a Monte-Carlo randomization test was completed for testing the null hypothesis of no-differences between observers (observations were randomly shifted between observers but constrained within an image). The ANOVAs were performed using the R software (R Foundation: www.r-project.org) and the *Vegan* package.

2.5.2. Data validation

We assessed the correspondence of the presence–absence of seagrass of the sampled photographs with a previously produced map. The *Posidonia*-LIFE map was built up by integrating side scan sonar, aerial photography and SCUBA observations (Fig. 1). We defined the seagrass presence at a location when the mean of the ACI values was equal to or higher than 0.5% (this requires having, in at least 2 out of 3 images, a BBCA score of 1). Before overlapping sampled locations with a polygonal map, we defined a buffer area of 15 m around each location, to consider the uncertainty associated with the GPS error. We used the kappa index of agreement (Cohen, 1960) to assess the reliability between observed values (i.e., sampled images) and expected values (i.e., benthic map). The kappa index varies between -1 and 1, where 1 indicates perfect agreement, −1 perfect disagreement, and 0 random assignment.

2.5.3. Spatial model

We implemented a predictive spatial model for point-referenced data of seagrass cover on the area of the MPA. Data used for the analysis only contained those locations where *P. oceanica* was present ($n = 64$). To assess the predictive performance of the model, we held out a randomly selected subset of 15% ($n = 10$ locations), for cross-validation. The predictive spatial model consisted of a Bayesian hierarchical model, as is implemented in the *spBayes* package (Finley et al., 2007).

The steps involved in the process are the following (see Appendix 1 for more details): (1) specifying a logistic regression model to relate environmental variables with seagrass cover; (2) defining a spatial correlation function to incorporate the spatial dependence in the model; (3) assigning prior distributions to set the probability distribution that represents the uncertainty of the model parameters; (4) using Markov Chain Monte Carlo (MCMC) methods to fit the model; and (5) sampling the posterior distribution to map the predicted values as well as the uncertainty of the predictions.

We then used the prediction on the random set-aside subset to measure the prediction error of the model (i.e., the cross-validated prediction error). We computed the root mean square error (RMSE). Finally, we also computed the RMSE for a non-spatial logistic regression on a generalized linear model, to compare the two models.

3. Results

3.1. Observer bias

After some training, there was no evidence of between-observed bias. An ANOVA demonstrated that between-observer differences were non-significant ($F = 0.0092$). The probability of obtaining this value when the null hypothesis [no differences between observers] is true is 0.53; this value is based on 1000 random permutations. Observers were freely permuted within images but images were not permuted.

3.2. Agreement between methodologies

P. oceanica was detected at locations deeper than 6 m (coinciding with the minimum sampled depth) and down to 33 m depth (maximum sampled depth was 35 m). Results from validation of seagrass presence–absence at sampled locations in relation to the *Posidonia*-LIFE map are presented in Table 2. In only one sample was *P. oceanica* not detected at a location where it was expected to appear, in accordance with the *Posidonia*-LIFE map. This sampled location was at 31.5 m depth, and the distance to the closest edge between seagrass and sandy bottoms was 85 m (based on the *Posidonia*-LIFE map). In contrast, we detected seagrass at 7 sampled locations where it was not expected to appear. Four of these 7 locations had very low seagrass cover (ACI < 2.5%) and were placed at the greatest depths, which were close to the lower limit. They were located near seagrass patches (at distances ranging between

Table 2
Presence–absence correspondence between current assessment and the Posidonia-LIFE map, which has been reclassified into presence and absence of *Posidonia oceanica*.

Sampling	Posidonia-LIFE map		Total
	Posidonia presence	Posidonia absence	
Posidonia presence	57	7	64
Posidonia absence	1	47	48
Total	58	54	112

Table 3
Coefficient estimates of a hierarchical spatial regression model (posterior medians and upper and lower 2.5 percentiles). First block provide point and credible interval estimates of the intercept and covariates. Second block provide estimates for the variance, spatial decay and effective range parameters.

Parameter	Posterior median	0.025 Quantile	0.975 Quantile
Intercept	9.20	1.59	18.61
Depth	−0.30	−0.60	−0.06
U_b	−13.86	−32.12	2.63
Slope	−0.71	−2.19	0.76
σ^2	0.164	0.060	0.620
ϕ	0.008	0.001	0.015
Effective range (m)	367	194	4207

17 and 110 m from the closest seagrass patch). The remaining 3 of the 7 locations had high seagrass cover (ACI = 87.5%) and corresponded in the *Posidonia*-LIFE map to *epilithic algae*. They were also located near seagrass patches (at distances ranging between 25 and 133 m from the closest seagrass patch), close to the upper limit. The kappa index based on Table 2 data was 0.86, which can be considered as very good (Landis and Koch, 1977).

3.3. Spatial distribution

Maps of the covariates used for model prediction are presented in Fig. 3. The depth ranged between 5.7 and 37.6 m, with a mean value of 24.4 m, while the slope ranged between 0.0 and 3.7 (%), with a mean value of 0.6 (%). The U_b ranged between 0.0 and 0.8 ms^{-1}, with a mean value of 0.07 ms^{-1}.

Parameter estimates of the spatial model are detailed in Table 3. The credible intervals (CI) suggested that depth significantly contributed to the model, whereas the U_b is significant at the 90% CI. *P. oceanica* cover would be negatively associated with depth and wave characteristics (Table 3). However, there was no significant effect of slope on seagrass cover (Table 3). The median values of spatial parameters are 0.164 for σ^2, and 0.008 for ϕ (see the specification of the spatial effect variance -σ^2- and the spatial decay parameter -ϕ- in Appendix 1). The posterior median of the effective range indicates a decline in the residual spatial autocorrelation at ∼350 m. The uncertainty of the latter parameter is relatively large (CI = 194–4207 m), which indicates that it cannot be estimated precisely.

In the probability map (Fig. 4a) the median value of each pixel's posterior distribution serves as the prediction. The predicted probability of seagrass cover is mainly driven by depth. Note also that in some areas (i.e., in the SE zone) of shallow waters there is a decrease of seagrass cover, possible due to high U_b. The prediction error is presented by the range of 0.025 and 0.975 CI quantiles (Fig. 4b). Cross-validation performance of the spatial model (RMSE 0.213) was similar to the model obtained by a non-spatial logistic model (RMSE 0.214).

4. Discussion

Vertical photography from a drop camera permits coverage of a large area and collects deeper samplings in comparison with conventional vertical photography conducted by scuba divers. Other applications for seagrass mapping have used similar drop-cameras (Bekkby et al., 2008; Roelfsema et al., 2009) and tow-camera systems (Stevens and Connolly, 2005; Holmes et al., 2007; Lefebvre et al., 2009). Holmes et al. (2007) stated that four main factors make image classification difficult: (1) camera angle; (2) proximity to plant; (3) conditions of light; and (4) water column turbidity. Our drop camera system successfully solved the first two factors, providing the same camera angle and distance to the seagrass for all of the images. Control over the conditions of lighting may be overcome with powerful lights and white balance correction, while water column turbidity constitutes an external factor that is more difficult to control. Nevertheless, these two factors are more relevant for species differentiation or automatic image classification and are not relevant for estimating seagrass cover in well identifiable seagrass meadows, as was our purpose. The estimation of seagrass cover was made by visual inspection and used a semi-quantitative scale that resulted in a rapid visual assessment technique. It is noticeable that, after some training with a small collection of reference images, no between-observer bias was detected.

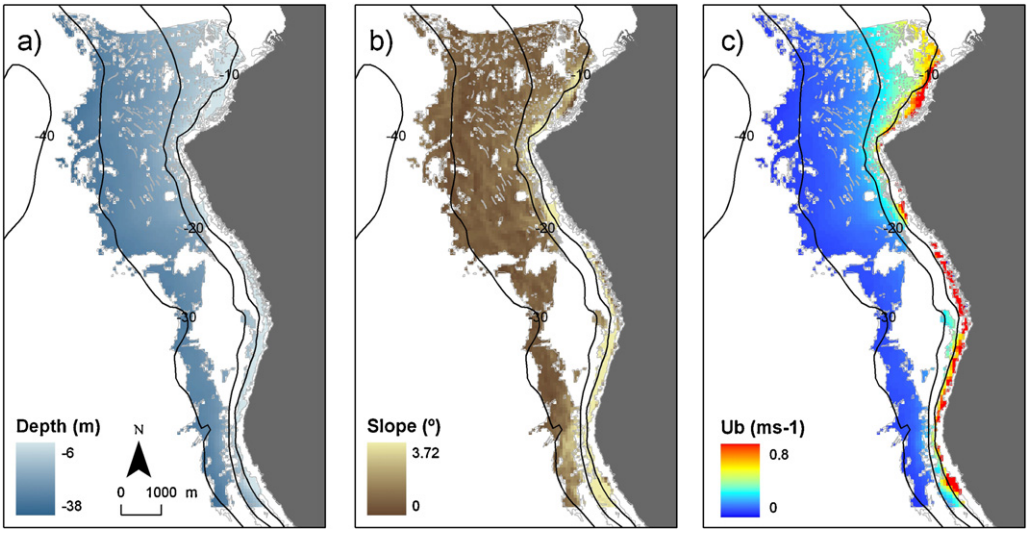

Fig. 3. Environmental covariates on vegetated areas (gridsize 15 m × 15 m). (a) bathymetry; (b) slope; (c) near-bottom orbital velocities (U_b).

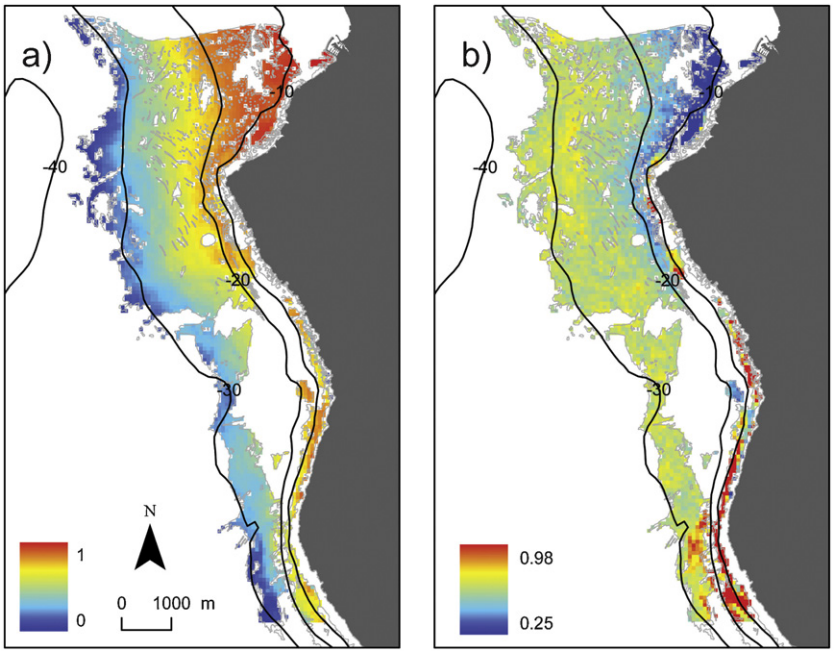

Fig. 4. Spatial prediction of seagrass cover (gridsize 75 m × 75 m): (a) posterior estimates (median) for predicted response surface Y(s) seagrass cover; (b) uncertainty of the prediction represented by the range between the lower and upper 95% posterior predictive intervals.

The relationship of seagrass spatial distribution with bathymetry, wave exposure and slope has been explored in previous studies (e.g. Kelly et al., 2001; Krause-Jensen et al., 2003; Zupo et al., 2006; Bekkby et al., 2008; Infantes et al., 2009). In our study, depth and wave exposure (as U_b) were significant, whereas slope had no effect on the seagrass cover. Depth was the most important factor that determined the spatial distribution of *P. oceanica* cover in our study area. This result is consistent with previous studies (Marbà et al., 2002; Zupo et al., 2006). However, in terms of its effects on seagrass cover, instead of a direct explanatory variable, depth should be considered as a proxy for light attenuation (Duarte, 1991; Dalla Via et al., 1998; Duarte et al., 2007). The lower depth limit found in our dataset of 33 m conforms with other sources on *P. oceanica* (Marbà et al., 2002; Zupo et al., 2006; Duarte et al., 2007).

The negative relationship of seagrass cover with wave exposition (decreasing cover with increasing wave exposition) has been also demonstrated in previous studies (Kelly et al., 2001; Fonseca et al., 2002; Krause-Jensen et al., 2003; Bekkby et al., 2008; Infantes et al., 2009). However, hydrodynamic conditions have been shown to have little influence on the meadow cover below the depth where wave action on the seafloor becomes negligible (Vacchi et al., 2010). In our study, we found a negative relationship between seagrass cover and U_b, as seagrass cover decreases with increasing near-bottom orbital velocities.

Slope has been identified as an important factor for the distribution of macrophytes (Duarte and Kalff, 1990; Narumalani et al., 1997; Bekkby et al., 2008). Plant biomass decreases with increasing slope, as steep slopes will limit the rooting capabilities of aquatic plants. However, any effects of slope have been found in many study areas with small slope variations in gentle terrains (Krause-Jensen et al., 2003). Our study area was similar to the latter case, which would explain the lack of significance of slope in our model.

Uncertainty maps can be used to detect regions where the number of observations should be increased. Our results suggest higher uncertainty near the upper limit of *P. oceanica*. This pattern could be due to the effect of waves in shallow waters. This effect could probably be better modeled if more locations in shallow waters were measured. In deeper water, the uncertainty increased too, probably due to the vicinity to the lower-limit, where density is reduced and beds become patchy.

Spatial dependence of the cover has been reported for other *Posidonia* species (Holmes et al., 2007; Kendrick et al., 2008). Holmes et al. (2007) determined spatial dependence for *Posidonia sinuosa* and *Posidonia coriacea* over more than 2500 m. Similarly, Kendrick et al. (2008) determined ranges over 610 m up to *ca.* 3 km. In our study, the extent of spatial dependence (effective range) is close to 350 m. However, this parameter has been estimated with low precision and it could reach up to *ca.* 4 km (upper 95% CI). Pairs of locations at <350 m represent 1.5% of this study, while those located at <4000 m represent 54.2%. The low number of pairs separated at <350 m would suggest a low effect of spatial autocorrelation on parameter estimation. This observation would explain the small difference in RMSE between the geostatistical model and the non-spatial model, and it suggests considerable homogeneity in bed cover.

Acknowledgements

This work would not have been possible without the help and support of the people that collaborated in the fieldwork, particularly M. Linde, I. Álvarez, S. Pérez, E. García, and J. Pericás. We thank Andrew Finley for support on spBayes. We also thank the support given by Albatros Marine Technologies SL, and Skua Gabinet d'Estudis Ambientals SLP. The habitat map was obtained from the Posidonia-LIFE program, Government of the Balearic Islands. This study was financed by the projects ROQUER (CTM2005-00283) and CONFLICT (CGL2008-958), which were funded by the Spanish Ministry of Research and Science. The authors D.M., J.A and E.I. had a fellowship from the Spanish Ministry of Research and Science, and M.C. from the Government of the Balearic Islands.

Appendix A. Supplementary data

Supplementary data associated with this article can be found, in the online version, at http://dx.doi.org/10.1016/j.aquabot.2012.12.005.

References

Álvarez-Ellacuria, A., Orfila, A., Olabarrieta, M., Medina, R., Vizoso, G., Tintoré, J., 2010. A nearshore wave and current operational forecasting system. J. Coast. Res. 26, 503–509.

Banerjee, S., Calin, B.P., Gelfand, A.E., 2004. Hierarchical Modeling and Analysis for Spatial Data. Chapman and Hall/CRC, Boca Raton.

Bekkby, T., Rinde, E., Erikstad, L., Bakkestuen, V., Longva, O., Christensen, O., Isaeus, M., Isachsen, P.E., 2008. Spatial probability modelling of eelgrass (*Zostera marina*) distribution on the west coast of Norway. ICES J. Mar. Sci. 65, 1093–1101.

Boudouresque, C.F., 1971. Méthodes d'etude qualitative et quantitative du benthos (en particulier du phytobenthos). Tethys 3, 79–104.

Boudouresque, C.F., Bernard, G., Pergent, G., Shili, A., Verlaque, M., 2009. Regression of Mediterranean seagrasses caused by natural processes and anthropogenic disturbances and stress: a critical review. Bot. Mar. 52, 395–418.

Cohen, J., 1960. A coefficient of agreement for nominal scales. Educ. Psychol. Meas. 20, 37–46.

Dalla Via, J., Sturmbauer, C., Schonweger, G., Sötz, E., Mathekowitsch, S., Stifter, M., Rieger, R., 1998. Light gradients and meadow structure in *Posidonia oceanica*: ecomorphological and functional correlates. Mar. Ecol. Prog. Ser. 163, 267–278.

Duarte, C.M., Kalff, J., 1990. Patterns in the submerged macrophyte biomass of lakes and the importance of scale of analysis in the interpretation. Can. J. Fish. Aquat. Sci. 47, 357–363.

Duarte, C.M., 1991. Seagrass depth limits. Aquat. Bot. 40, 363–377.

Duarte, C.M., Marbà, N., Krause-Jensen, D., Sánchez-Camacho, M., 2007. Testing the predictive power of seagrass depth limit models. Estuaries Coasts 30, 652–656.

Finley, A., Banerjee, S., Carlin, B.P., 2007. spBayes: an R package for univariate and multivariate hierarchical point-referenced spatial models. J. Stat. Softw. 19, 1–24.

Fonseca, M., Whitfield, P.E., Kelly, N.M., Bell, S.S., 2002. Modeling seagrass landscape pattern and associated ecological attributes. Ecol. Appl. 12, 218–237.

Fourqurean, J.W., Willsie, A., Rose, C.D., Rutten, L.M., 2001. Spatial and temporal pattern in seagrass community composition and productivity in south Florida. Mar. Biol. 138, 341–354.

Fourqurean, J.W., Boyer, J.N., Durako, M.J., Hefty, L.N., Peterson, B.J., 2003. Forecasting responses of seagrass distributions to changing water quality using monitoring data. Ecol. Appl. 13, 474–489.

Fourqurean, J.W., Marba, N., Duarte, C.M., Diaz-Almela, E., Ruiz-Halpern, S., 2007. Spatial and temporal variation in the elemental and stable isotopic content of the seagrasses *Posidonia oceanica* and *Cymodocea nodosa* from the Illes Balears. Spain. Mar. Biol. 151, 219–232.

Grech, A., Coles, R.G., 2010. An ecosystem-scale predictive model of coastal seagrass distribution. Aquat. Conserv.-Mar. Freshw. Ecosyst. 20, 437–444.

Holmes, K.W., Van Niel, K.P., Kendrick, G.A., Radford, B., 2007. Probabilistic large-area mapping of seagrass species distributions. Aquat. Conserv.-Mar. Freshw. Ecosyst. 17, 385–407.

Infantes, E., Terrados, J., Orfila, A., Cañellas, B., Álvarez-Ellacuria, A., 2009. Wave energy and the upper depth limit distribution of *Posidonia oceanica*. Bot. Mar. 52, 419–427.

Infantes, E., Orfila, A., Tjeerd, B.J., Simarro, G., Terrados, J., 2011. *Posidonia oceanica* and *Cymodocea nodosa* seedling tolerance to wave exposure. Limnol. Oceanogr. 56, 2223–2232.

Infantes, E., Orfila, A., Simarro, G., Terrados, J., Luhar, M., Nepf, H., 2012. Effect of a seagrass (*Posidonia oceanica*) meadow on wave propagation. Mar. Ecol. Prog. Ser. 456, 63–72.

Jordan, A., Lawler, M., Halley, V., Barrett, N., 2005. Seabed habitat mapping in the Kent Group of islands and its role in marine protected area planning. Aquat. Conserv.-Mar. Freshw. Ecosyst. 15, 51–70.

Kelly, N.M., Fonseca, M., Whitfield, P., 2001. Predictive mapping for management and conservation of seagrass beds in North Carolina. Aquat. Conserv.-Mar. Freshw. Ecosyst. 11, 437–451.

Kendrick, G.A., Karen, W.H., Kimberly, P.V.N., 2008. Multi-scale spatial patterns of three seagrass species with different growth dynamics. Ecography 31, 191–200.

Kirby, J.T., Dalrymple, R.A., 1983. The propagation of weakly nonlinear waves in the presence of varying depth and currents. In: Proc. XXth Congress I.A.H.R, Moscow.

Krause-Jensen, D., Pedersen, M., Jensen, C., 2003. Regulation of eelgrass (*Zostera marina*) cover along depth gradients in Danish coastal waters. Estuaries Coasts 26, 866–877.

Landis, J.R., Koch, G.G., 1977. The measurement of observer agreement for categorical data. Biometrics 33, 159–174.

Lefebvre, A., Thompson, C.E.L., Collins, K.J., Amos, C.L., 2009. Use of a high-resolution profiling sonar and a towed video camera to map a *Zostera marina* bed, Solent, UK. Estuar. Coast. Shelf Sci. 82, 323–334.

Leriche, A., Boudouresque, C.-F., Monestiez, P., Pasqualini, V., 2011. An improved method to monitor the health of seagrass meadows based on kriging. Aquat. Bot. 95, 51–54.

Marbà, N., Duarte, C.M., 1998. Rhizome elongation and seagrass clonal growth. Mar. Ecol. Prog. Ser. 174, 269–280.

Marbà, N., Duarte, C.M., Holmer, M., Martínez, R., Basterretxea, G., Orfila, A., Jordi, A., Tintoré, J., 2002. Effectiveness of protection of seagrass (*Posidonia oceanica*) populations in Cabrera National Park (Spain). Environ. Conserv. 29, 509–518.

Narumalani, S., Jensen, J.R., Anthausen, J.D., Burkhalter, J.D., Mackey, S., 1997. Aquatic macrophyte modelling using GIS and logistic multiple regression. Photogramm. Eng. Remote Sens. 63, 41–49.

Roelfsema, C.M., Phinn, S.R., Udy, N., Maxwell, P., 2009. An integrated field and remote sensing approach for mapping seagrass cover, Moreton Bay, Australia. J. Spat. Sci. 54, 45–62.

Stevens, T., Connolly, R.M., 2005. Local-scale mapping of benthic habitats to assess representation in a marine protected area. Mar. Freshw. Res. 56, 111–123.

Vacchi, M., Montefalcone, M., Bianchi, C.N., Morri, C., Ferrari, M., 2010. The influence of coastal dynamics on the upper limit of the *Posidonia oceanica* meadow. Mar. Ecol. 31, 546–554.

van der Maarel, E., 1979. Transformation of cover-abundance values in phytosociology and its effect on community similarity. Vegetation 39, 97–114.

Zupo, V., Mazzella, L., Buia, M.C., Gambi, M.C., Lorenti, M., Scipione, M.B., Cancemi, G., 2006. A small-scale analysis of the spatial structure of a *Posidonia oceanica* meadow off the Island of Ischia (Gulf of Naples, Italy): relationship with the seafloor morphology. Aquat. Bot. 84, 101–109.